Simple Model for Piezoelectric Ceramic/Polymer 1–3 Composites Used in Ultrasonic Transducer Applications

HELEN LAI WAH CHAN AND JOSEPH UNSWORTH, SENIOR MEMBER, IEEE

Abstract—**A theoretical model is presented for combining parameters of 1–3 ultrasonic composite materials so as to be able to predict ultrasonic characteristics such as velocity, acoustic impedance, electromechanical coupling factor and piezoelectric coefficients. Hence the model allows the estimation of resonance frequencies of 1–3 composite transducers.**

I. Introduction

A VARIETY of composite piezoelectric materials can be made by combining a piezoelectric ceramic with a passive polymer. These composites are classified according to their connectivity [1]. The 1–3 piezoelectric ceramic/polymer composites have been used as transducers for pulse–echo medical ultrasonic imaging [2]–[5]. The properties of these 1–3 composites can be tailored [5] to combine the desired properties of high thickness electromechanical coupling constants (k_t = 0.6 to 0.70) and low acoustic impedance ($Z < 7.5$ Mrayl). They also provide a wide range of dielectric constants (ϵ/ϵ_0 = 10 to 1000) and low dielectric and mechanical losses, which are useful in electronic circuit constructions.

The thickness mode resonance is the resonance of practical interest for ultrasonic pulse–echo type transducer applications. The lateral spatial scale determines whether the material behaves in a homogeneous manner, if the lateral periodicity d is small the composite will have new effective materials constants.

A theoretical model for the calculation of new material parameters of PZT/polymer 1–3 composites having fine lateral periodicity has been developed by Smith *et al.* [5]. This model follows the parallel connectivity approach [6], [7] used to calculate composite properties. Comparison between thickness resonance parameters determined from Smith's model and measured values of PZT 5A/Spurr Epoxy 1–3 composites of PZT volume fraction ν up to 0.4 yielded good agreement.

We have extended this model to cover more material parameters and compared them with experimental results up to PZT volume fraction ν of 0.8. The model also covers calculation of piezoelectric charge constants d_{33} and d_{31}. Values are then found to be in good agreement with experimental results obtained for PZT 7A/Araldite D 1–3 composites which we have fabricated. Acoustic velocity, acoustic impedance and electromechanical coupling factor are also predicted and found to be close to the values determined experimentally. d_h values of PZT 5A/Spurr epoxy composites are also calculated and agreed with published results [7].

II. Assumptions and Validity of the Model

The following assumptions have been adopted in the model calculations.

1) Equal strains in the vertical directions as

$$\bar{S}_3 = S_3^P = S_3^C, \qquad \bar{T}_3 = \nu T_3^C + (1 - \nu) T_3^P$$

where $\bar{S}_3$, $\bar{T}_3$, S_3^P T_3^P, S_3^C, and T_3^C are the vertical strains and stresses in the composite, polymer and ceramic respectively. This is essentially equivalent to the Voigt model isostrain assumption. This assumption is true when either a) or b) is satisfied.

a) The composite has a fine spatial scale so that the lateral stopband resonances are at much higher frequencies than the thickness resonance i.e., when there is no mode coupling [5].

b) The composite is thick so the thickness mode is still separated from the lateral stopband resonance. Furthermore, the polymer can be considered as effectively tied to the ceramic if the polymer width is small compared to the shear wavelength at the driving frequency [2]. The plate will oscillate uniformly with equal strain in both phases only when this is satisfied. Note that this imposes a limit only on the width of the polymer, therefore the isostrain assumption should be valid for thick 1–3 composites with large rod size but with small polymer width (e.g., 1 mm wide ceramic with 75-μm polymer width).

2) The electric fields are taken to be the same in both

Manuscript received April 17, 1987; accepted February 23, 1988. This work was supported by the Australian Research Grant Scheme and the Australian Institute of Nuclear Science and Engineering.

H. Chan is with CSIRO Division of Applied Physics, National Measurement Laboratory, Institute of Industrial Technologies, Bradfield Road, West Lindfield, New South Wales 2070, Australia.

J. Unsworth is with the School of Mathematics, Physics, Computing, and Electronics, Macquarie University, Sydney, New South Wales 2109, Australia.

IEEE Log Number 8927874.

phases, namely as

$$\bar{E}_3 = E_3^P = E_3^C, \quad \text{and} \quad \bar{E}_1 = \bar{E}_2 = 0$$

where $\bar{E}_3$, E_3^P, and E_3^C are the electric fields in the vertical direction for the composite, polymer, and ceramic, respectively, and where $\bar{E}_1$, $\bar{E}_2$, and $\bar{E}_3$ are the electric fields in the x, y, and z direction, respectively. This is true only if all fringing fields are neglected.

3) The lateral stresses are assumed to be equal in both phases and that any lateral strain in the ceramic is compensated by a complimentary strain in the polymer. The composite as a whole is laterally clamped since the thickness resonance frequency will be operated at high frequencies compared with planar modes of the sample. However, the individual phases have lateral scales corresponding to higher frequencies than the thickness resonances so that the substructure is not laterally clamped.

We have

$$\bar{T}_1 = T_1^P = T_1^C, \qquad \bar{S}_1 = (1 - \nu)S_1^P + \nu S_1^C = 0$$

and

$$\bar{T}_1 = \bar{T}_2, \bar{S}_1 = \bar{S}_2$$

because of symmetry in x-y plane where $\bar{T}_1$, $\bar{S}_1$, T_1^P, S_1^P, and T_1^C, S_1^C are the stress and strain in the x direction in the composite, polymer and ceramic respectively.

This assumption is equivalent to a series model in the x and y direction where isostress condition has been assumed. It is only an approximation since there is discontinuity in stress on the outside boundaries of the composite plate.

4) The effective dielectric displacement $\bar{D}_3$ is obtained by averaging over the contributions of the two phases as

$$\bar{D}_3 = \nu D_3^C + (1 - \nu)D_3^P$$

where D_3^C and D_3^P are the dielectric displacements in the ceramic and polymer phase.

This is satisfied when the isostrain condition in the vertical direction is true, namely, the polymer width is small enough so that the charge density on the surface is uniform.

III. Equations for 1-3 Composite Material Parameters

The detailed mathematical analysis can be found elsewhere [5], [8], and the final derived equations only for the calculations of 1-3 composite material parameters are presented here. It is noted that subscripts 1 and 3 denote x- and z-axes, superscript P denotes polymer phase. Quantities with superscripts C, E, D, S and T are material parameters of the ceramic and those with bars e.g., $\bar{d}_{33}$, $\bar{C}_{33}^E$ are composite material constants.

For meaning of C_{33}^E, e_{33} and ϵ_{33}^T, etc., please refer to the list of symbols in the IRE standard [9]. Let ν be the volume fraction of PZT in the composite and let

$$C(\nu) = C_{11}^E + C_{12}^E + \nu(C_{11}^P + C_{12}^P)/(1 - \nu)$$

where C_{11}^P and C_{11}^E are the stiffness constants of the polymer and ceramic.

$$\bar{C}_{33}^E = \nu\left[C_{33}^E - 2(C_{13}^E - C_{12}^P)^2/C(\nu)\right] + (1 - \nu)\, C_{11}^P \tag{1}$$

$$\bar{e}_{33} = \nu\left[e_{33} - 2e_{31}(C_{13}^E - C_{12}^P)/C(\nu)\right] \tag{2}$$

$$\bar{\epsilon}_{33}^S = \nu\left[\epsilon_{33}^S + 2(e_{21})^2/C(\nu)\right] + (1 - \nu)\epsilon_{11}^P \tag{3}$$

$$\bar{C}_{13}^E = \left[C_{12}^P(C_{11}^E + C_{12}^E) + \nu\, C_{13}^E(C_{11}^P + C_{12}^P)/(1 - \nu)\right]/C(\nu) \tag{4}$$

$$\bar{e}_{31} = e_{31}\left[1 - (C_{11}^E + C_{12}^E)/C(\nu)\right]. \tag{5}$$

Let $s(\nu) = \nu s_{11}^P + (1 - \nu)s_{33}^E$ where s_{11}^P and s_{33}^E are the compliances of polymer and ceramic

$$\bar{s}_{13}^E = \left[s_{33}^E s_{12}^P(1 - \nu) + \nu s_{11}^P s_{13}^E\right]/s(\nu) \tag{6}$$

$$\bar{s}_{33}^E = \frac{s_{11}^P s_{33}^E}{s(\nu)} \tag{7}$$

$$\bar{d}_{33} = \nu s_{11}^P d_{33}^C/s(\nu) \tag{8}$$

$$\bar{d}_{31} = \nu d_{31}^C - \nu(1 - \nu)\, d_{33}^C(s_{13}^E - s_{12}^P)/s(\nu) \tag{9}$$

$$\bar{\epsilon}_{33}^T = \nu\epsilon_{33}^T - \nu(1 - \nu)\,(d_{33}^C)^2/s(\nu) + (1 - \nu)\epsilon_{11}^P \tag{10}$$

$$\bar{s}_{11}^E + \bar{s}_{12}^E = \left[\nu(s_{11}^E + s_{12}^E) + (1 - \nu)\,(s_{11}^P + s_{12}^P) - 2\nu(1 - \nu)\,(s_{13}^E - s_{12}^P)^2/s(\nu)\right] \tag{11}$$

$$\bar{\rho} = \nu\rho^C + (1 - \nu)\rho^P. \tag{12}$$

From the previously mentioned equations, the following parameters can be calculated [10]:

$$\bar{\beta}_{33}^S = 1/\bar{\epsilon}_{33}^S \tag{13}$$

$$\bar{C}_{33}^D = \bar{C}_{33}^E + (\bar{e}_{33})^2\,\bar{\beta}_{33}^S \tag{14}$$

$$\bar{h}_{33} = \bar{e}_{33}\bar{\beta}_{33}^S \tag{15}$$

$$\bar{C}_{13}^D = \bar{C}_{13}^E + \bar{e}_{33}\bar{e}_{31}\bar{\beta}_{33}^S \tag{16}$$

$$\bar{h}_{31} = \bar{e}_{31}\bar{\beta}_{33}^S \tag{17}$$

$$\bar{k}_t = (1 - \bar{C}_{33}^E/\bar{C}_{33}^D)^{1/2} \tag{18}$$

$$\bar{k}_p = (1 - \bar{\epsilon}_{33}^S\,\bar{C}_{33}^D/\bar{\epsilon}_{33}^T\,\bar{C}_{33}^E)^{1/2}. \tag{19}$$

The longitudinal velocity is

$$\bar{V}_3^D = (\bar{C}_{33}^D/\bar{\rho})^{1/2} \tag{20}$$

and the specific acoustic impedance is

$$\bar{Z} = \bar{\rho}\bar{V}_3^D. \tag{21}$$

It is noted that these equations lead to correct limiting values when $\nu = 0$ and $\nu = 1$.

The hydrostatic coefficient is given by

$$\bar{d}_h = \left[\nu s_{11}^P - 2\nu(1-\nu)(s_{13}^E - s_{12}^P)\right] d_{33}^C / \nu s_{11}^P + (1-\nu)s_{33}^E \left] d_{33}^C + 2d_{31}^C \nu. \quad (22)$$

IV. Theoretical Predictions for PZT7A/Aradite D Composites

To illustrate how the composite material parameters vary with volume fraction of piezoelectric ceramic, the material parameters of PZT 7A and Araldite D are used. They are listed in Table I.

The basic material parameters of the composite are shown in Fig. 1 to 9. Predictions of the theoretical curves are as follows.

1) The density $\bar{\rho}$ varies linearly with volume fraction ν of PZT.

2) $\bar{\epsilon}_{33}^S$ and $\bar{\epsilon}_{33}^T$ vary essentially linearly with ν except when ν is very small. This is because the dielectric constant of the polymer $\bar{\epsilon}_{11}^P$ is small compared to that of the ceramic and its contribution to the overall dielectric constant value is negligible when ceramic volume fraction is high.

3) $\bar{C}_{33}^E$ varies linearly w.r.t. ν for $\nu < 0.7$. If we examine (1), we would find

$$\bar{C}_{33}^E = \nu\left[C_{33}^E - 2(C_{13}^E - C_{12}^P)/C(\nu)\right] + (1-\nu)C_{11}^P \quad (22a)$$

$$= \nu C_{33}^{E'} + (1-\nu)C_{11}^P \quad (23)$$

The polymer contribution (second term) is quite small and the rod inside the composite can be considered to have an effective stiffness constant $C_{33}^{E'}$ where

$$C_{33}^{E'} = C_{33}^E - 2(C_{13}^E - C_{12}^P)^2/C(\nu) \quad (24)$$

and

$$C(\nu) = C_{11}^E + C_{12}^E + \nu(C_{11}^P + C_{12}^P)/(1-\nu). \quad (25)$$

In the term $2(C_{13}^E - C_{12}^P)^2/C(\nu)$ in (24), the presence of C_{11}^P and C_{12}^P represent the reduction of the stiffness due to polymer clamping. It stays quite constant for small ν since C_{11}^P and C_{12}^P are much smaller than C_{11}^E and C_{12}^E. This gives the initial linear dependance of $\bar{C}_{33}^E$ on ν. As ν increases, the clamping increases the stiffness to the value for a solid ceramic disc.

4) The strain constant $\bar{e}_{33}$ also varies linearly with respect to ν and from (2) we find

$$\bar{e}_{33} = \nu\left[e_{33} - 2e_{31}(C_{13}^E - C_{12}^P)/C(\nu)\right] \cong \nu\left[e_{33} - 2e_{31}C_{13}^E/(C_{11}^E + C_{12}^E)\right] = \nu e_{33}' \quad (26)$$

where

$$e_{33}' = e_{33} - 2e_{31}C_{13}^E/(C_{11}^E + C_{12}^E). \quad (27)$$

TABLE I
Material Parameters of PZT 7A [12] and Araldite D

PZT 7A			
C_{11}^E (10^{10} N/m^2)	14.80	$\epsilon_{33}^S/\epsilon_0$	235
C_{12}^E (10^{10} N/m^2)	7.62	$\epsilon_{33}^T/\epsilon_0$	425
C_{13}^E (10^{10} N/m^2)	7.42	ρ (kg/m^3)	7600
C_{33}^E (10^{10} N/m)	13.10	s_{11}^E (10^{-12} m^2/N)	10.7
C_{33}^D (10^{10} N/m^2)	17.50	s_{12}^E (10^{-12} m^2/N)	−3.2
C_{13}^D (10^{10} N/m^2)	7.30	s_{13}^E (10^{-12} m/N)	−4.6
e_{33} (C/m^2)	9.50	s_{33}^E (10^{-12} m/N)	13.9
e_{31} (C/m^2)	−2.10	k_t	0.50
d_{31} (10^{-12} m/V)	−60	k_{33}	0.66
d_{33} (10^{-12} m/V)	150	k_p	0.51
		V_3^D (m/s)	4800
Araldite D			
V_e (m/s)	2603	C_{12}^P (10^{10} N/m^2)	0.44
V_s (m/s)	1218	s_{11}^P (10^{-12} m^2/N)	216
ρ (kg/m^3)	1150	s_{12}^P (10^{-12} m^2/N)	−78
C_{11}^P (10^{10} N/m^2)	0.80	ϵ/ϵ_0	4

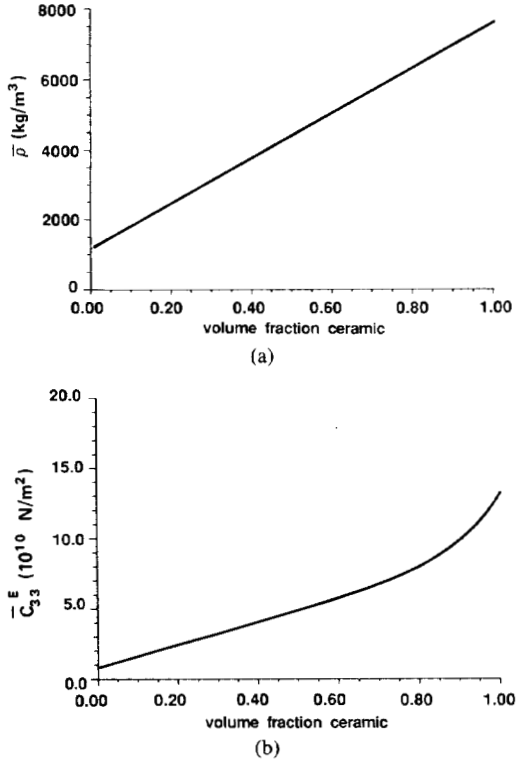

Fig. 1. (a) Variation of density $\bar{\rho}$ with volume fraction of PZT. (b) Variation of stiffness $\bar{C}_{33}^E$ with volume fraction of PZT.

When ν is large, the second term of [27] vanishes and e_{33} stops to increase and becomes e_{33} of the ceramic disc.

5) The derived results of the charge constant $\bar{d}_{33}$ is similar to that of the parallel model results used by Skinner and Klicker [6], [7]. This is not unexpected because similar assumptions have been used in the calculations. It is noted that from (8) and $s(\nu) = \nu s_{11}^P + (1-\nu)s_{33}^E$ gives

$$\bar{d}_{33} = \nu d_{33}^C / \left[\nu + (1-\nu)(s_{33}^E/s_{11}^P)\right]$$

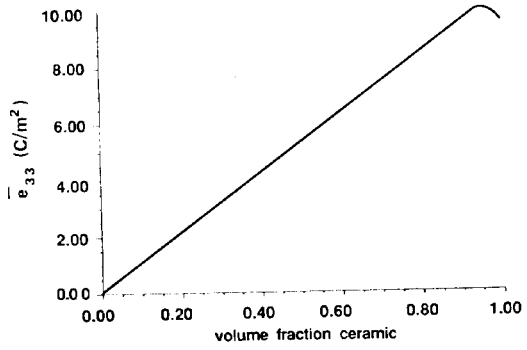

(a)

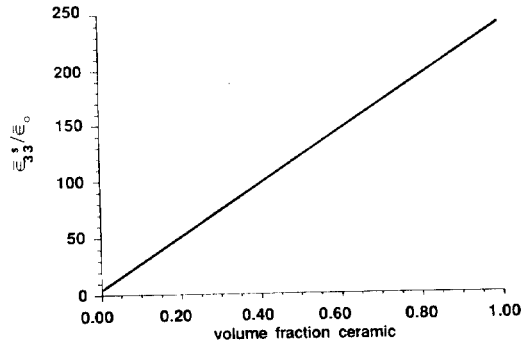

(b)

Fig. 2. (a) Variation of piezoelectric constant $\bar{e}_{33}$ with volume fraction of PZT. (b) Variation of relative dielectric constant $\bar{\epsilon}_{33}^{S}/\epsilon_0$ with volume fraction of PZT.

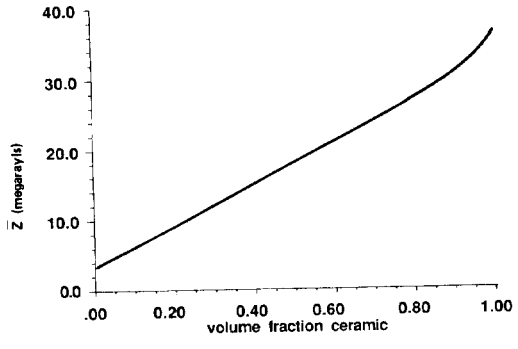

(a)

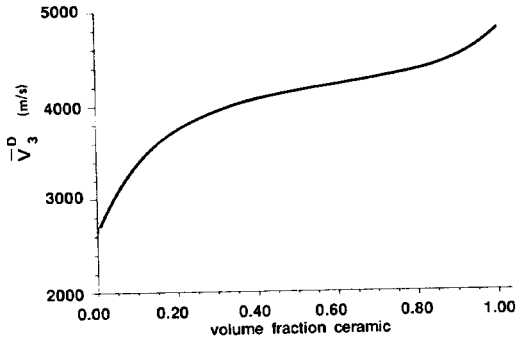

(b)

Fig. 4. (a) Variation of acoustic impedance $\bar{Z}$ with volume fraction of PZT. (b) Variation of longitudinal velocity $\bar{V}_3^D$ with volume fraction of PZT.

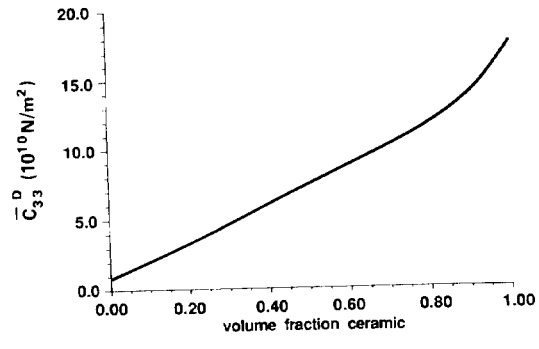

(a)

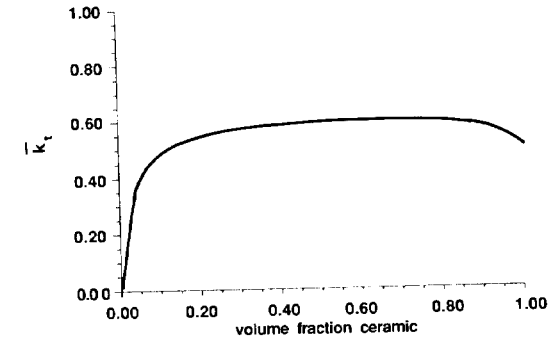

(b)

Fig. 3. (a) Variation of stiffness constant $\bar{C}_{33}^{D}$ with volume fraction of PZT. (b) Variation of thickness coupling constant $\bar{k}_t$ with volume fraction of PZT.

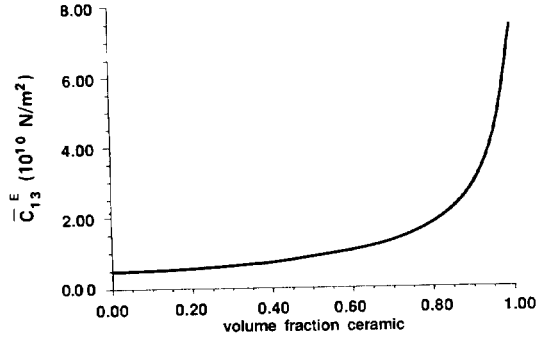

(a)

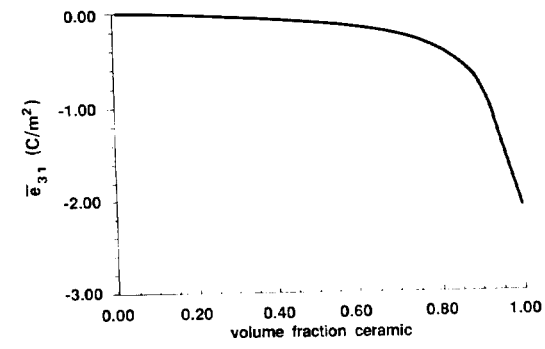

(b)

Fig. 5. (a) Variation of stiffness constant $\bar{C}_{13}^{E}$ with volume fraction of PZT. (b) Variation of piezoelectric constant $\bar{e}_{31}$ with volume fraction of PZT.

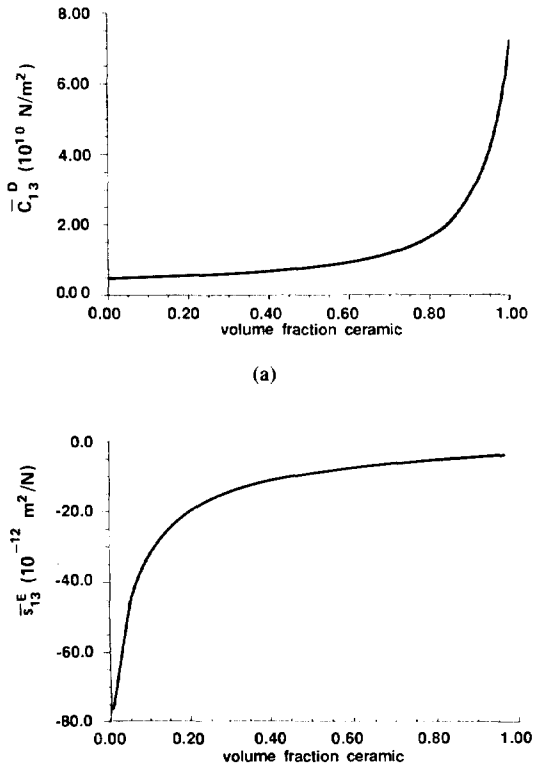

Fig. 6. (a) Variation of stiffness constant $\bar{C}^D_{13}$ with volume fraction of PZT. (b) Variation of compliance $\bar{s}^E_{13}$ with volume fraction of PZT.

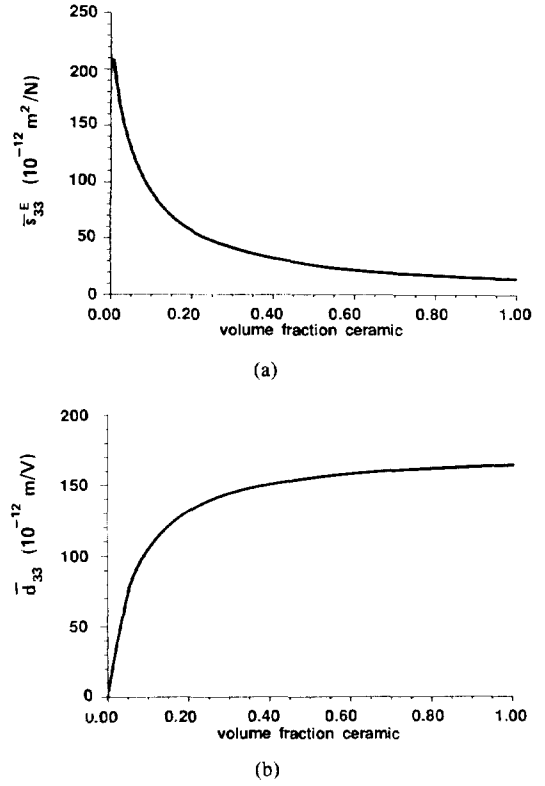

Fig. 7. (a) Variation of compliance $\bar{s}^E_{33}$ with volume fraction of PZT. (b) Variation of charge constant $\bar{d}_{33}$ with volume fraction of PZT.

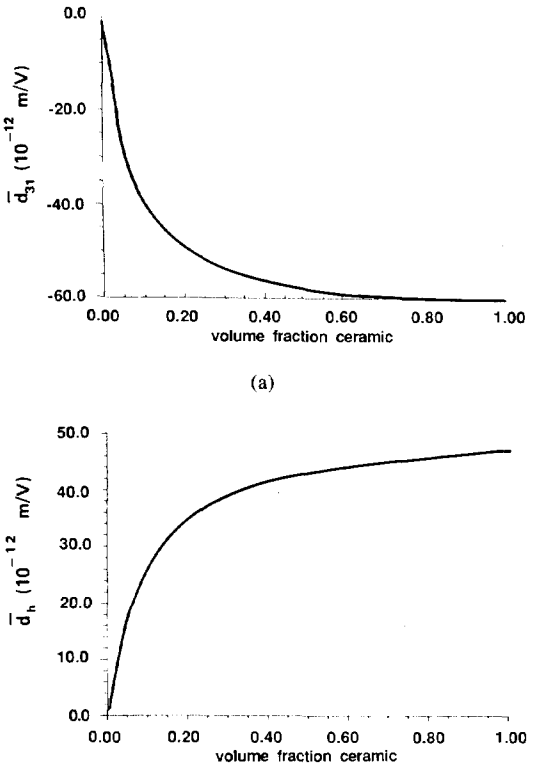

Fig. 8. (a) Variation of charge constant $\bar{d}_{31}$ with volume fraction of PZT. (b) Variation of hydrostatic charge constant $\bar{d}_h$ with volume fraction of PZT.

so a polymer with higher s^P_{11} (i.e., softer) will give a higher $\bar{d}_{33}$ value.

6) On the other hand from (22)

$$\bar{d}_h = \left[\nu s^P_{11} - 2\nu(1-\nu)\,(s^E_{13} - s^P_{12})\right]/d^C_{33}/\nu s^P_{11} + (1-\nu)s^E_{33}\Big] + 2d^C_{31}\nu$$

which is similar to that derived by Shorrocks *et al.* [11].

It can be seen that the closer s^P_{12} is to s^E_{13} of the ceramic (i.e., very small s^P_{12} is desired), the larger $\bar{d}_h$ becomes. This would imply that a polymer with small Poisson's ratio ($\sigma = -s^P_{12}/s^P_{11}$) is desirable. In practice, to achieve high s^P_{11} and small s^P_{12}, very often a third and fourth phase (e.g., microballoons and fiberglass) [11] has to be incorporated into a soft polymer matrix (e.g., Eccogel). In fact, in a well-decoupled and well-designed composite hydrophone, the value of $\bar{d}_h$ can be much higher than that calculated by the theory.

Fig. 8(b) shows $\bar{d}_h$ versus PZT volume fraction. It can be seen that PZT 7A combined with Araldite D would not make a good hydrophone, because Araldite D has relative small s^P_{11} and $\sigma = 0.36$ so s^P_{12} is quite large. Also $|s^E_{13}|$ of PZT 7A is the smallest among all the different types of ceramics [12]. Hence, the resulting $\bar{d}_h$ stays smaller than d_h of the ceramic for all ν. However, if PZT 5A and Spurr Epoxy 1-3 composite is used as another illustrative example, the small theory will predict a maximum $\bar{d}_h$ =

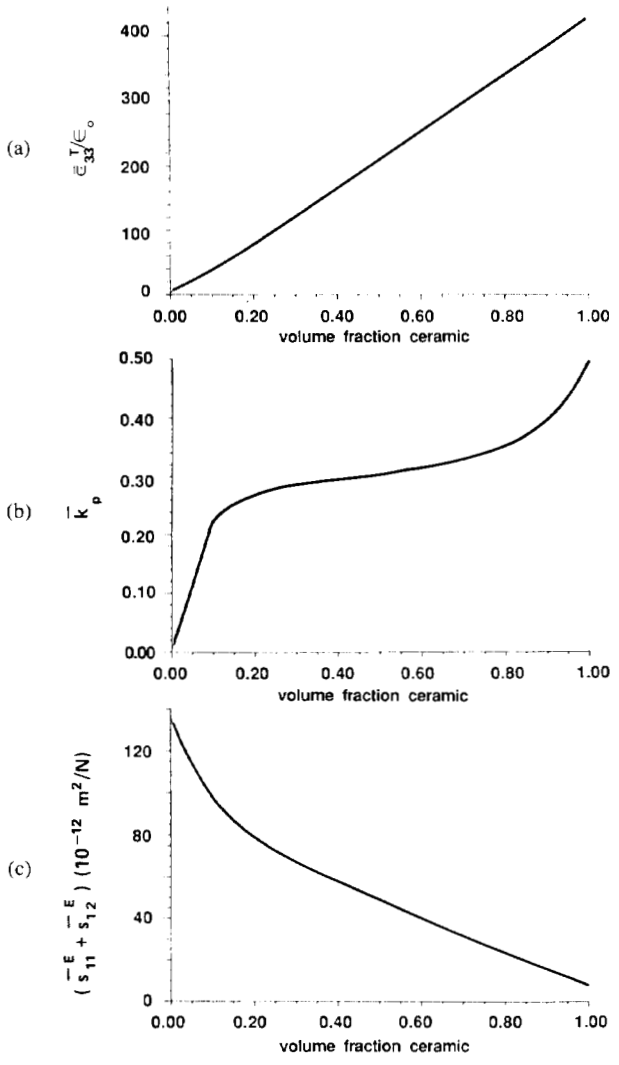

Fig. 9. (a) Variation of relative dielectric constant $\bar{\epsilon}_{33}^{T}/\epsilon_0$ with volume fraction of PZT. (b) Variation of planar coupling constant $\bar{k}_p$ with volume fraction of PZT. (c) Variation of compliances $\bar{s}_{11}^{E} + \bar{s}_{12}^{E}$ with volume fraction of PZT.

109×10^{-12} m/V at 0.25 PZT volume fraction. In the next section, the theoretical curve of PZT 5A/Spurr Epoxy 1–3 composites would be compared to the published result from Pennsylvania State University by K. A. Klicker [7].

7) It is difficult to derive $\bar{s}_{11}^{E}$ and $\bar{s}_{12}^{E}$ separately because of symmetry in the x-y plane, only $\bar{s}_{11}^{E} + \bar{s}_{12}^{E}$) can be calculated and compared to the values obtained from the planar mode resonance of the composite discs.

8) Other useful transducer parameters $\bar{Z}$, $\bar{V}_3^D$ and $\bar{k}_t$ are shown in Figs. 3 and 4, respectively. Essentially, the acoustic impedance Z increases linearly with ν except at large ν where clamping of the rods causes it to increase more rapidly. The presence of ceramic rod has a stiffening effect and causes the velocity to increase quite rapidly when ν increases from 0 to 0.2, as the ceramic fraction increases, the velocity increases only slowly. It is because although the stiffness increases due to adding of more ceramic, the density also increases, which leads to $\bar{V}_3^D = (\bar{C}_{33}^D/\bar{\rho})^{1/2}$. The mass loading tends to slow down the velocity increase. The velocity rises more rapidly at high values of ν due to the stiffening of the rods by the lateral forces exerted by the polymer.

9) The predicted electromechanical coupling constant $\bar{k}_t$ is nearly but lower than the k_{33} of free ceramic rods except for deviation at low- and high-volume fraction. It seems to be a good approximation to take $\bar{k}_t$ for the composite to be just the k_{33} constant of a free PZT rod.

10) The planar coupling constant $\bar{k}_p$ stays quite constant at about 0.3, which is much lower than k_p of the ceramic (0.51). The low $\bar{k}_p$ is an advantage of using composite in medical beam transducer fabrication. The grating side lobes will be reduced and a better quality image can be obtained.

V. Sample Fabrication and Measurements

The 1–3 composites are fabricated using dice-and-fill technique [4]. PZT 7A from Vernitron and Araldite D with hardener HY951 from Ciba Geigy are used. The ceramic is diced at AWA Aust. Pty. using an integrating wafering saw, the diamond saw blade width is 75 μm. Ceramic width of different composites are 80 μm, 0.15 mm, 0.22 mm, 0.30 mm, 0.45 mm, 0.60 mm, 0.75 mm, and 1 mm to cover a range of PZT volume fraction up to 0.82. (Fig. 10). To reduce breakage, the composite with 80 μm ceramic width is cut one way into thin strips, vacuum impregnated with polymer; after the polymer is cured, it is then cut perpendicularly. The ceramic is poled before dicing; hence poling is not required afterwards.

Air-dried silver (Du Pont 4817) is painted on as electrodes. The electric impedance as a function of frequency for each sample is measured using an impedance analyser Hewlett Packard Model HP 4192A interfaced to a computer HP 85 and plotting system HP 7090A. Values of $\bar{s}_{11}^{E}$, $\bar{s}_{12}^{E}$, $\bar{k}_p$, $\bar{k}_t$, and $\bar{V}_3^D$ ($=2N_t = 2f_n t$, where f_n is the frequency of maximum electric impedance and t is the sample thickness) are evaluated using the IEEE Standard [13]. Density of the samples are found using the Archimedes' Principle and checked by volume and weight measurements. Volume fraction ν is calculated using

$$\bar{\rho} = \nu\rho^C + (1 - \nu)\rho^P$$

Charge constant $\bar{d}_{33}$ of the composites are measured using the Berlincourt d_{33} meter (Channel Product Inc.).

VI. Comparison Between Predicted and Experimental Results

The PZT 7A/Araldite D samples have a 75-μm-polymer-column width with ceramic column widths ranging from 80 μm to 1 mm. The composite discs are 14 mm in diameter and ground to 1.2 mm thick. All the planar and thickness mode resonance parameters are determined and plotted together with the theoretical curves in Figs. 11–14.

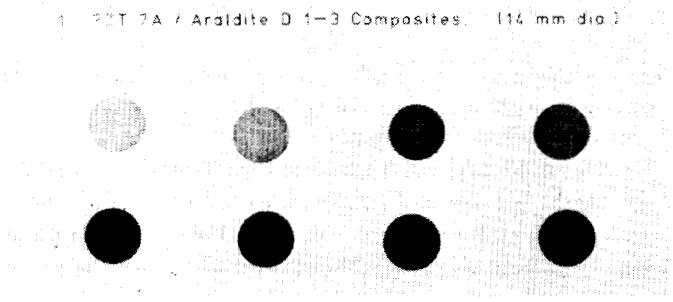

Fig. 10. PZT7A/Araldite D 1-3 composites.

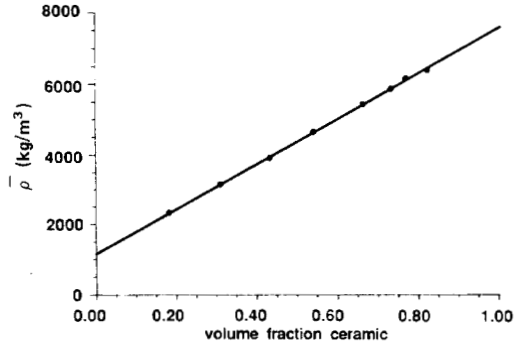

(a)

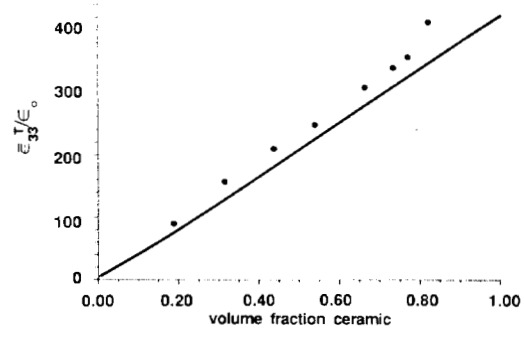

(b)

Fig. 11. (a) Experimental verification of variation of density $\bar{\rho}$ with volume fraction of ceramic (b) Experimental verification of variation of relative dielectric constant $\bar{\epsilon}_{33}^{T}/\epsilon_0$ with volume fraction of ceramic.

The experimental results of $\bar{\epsilon}_{33}^{T}/\epsilon_0$, $\bar{Z}$, $\bar{d}_{33}$, and $\bar{V}_3^D$ show essentially the same trend as predicted by the theory, the difference arises due to the fact that the theoretical curves are calculated using the manufacturer's data. Batch to batch variations can be quite large. For example, d_{33} for PZT 7A is given in the data sheet to be 150×10^{-12} m/V, but the measured value for a randomly chosen 7A ceramic sample is $163\text{–}167 \times 10^{-12}$ m/V. In Fig. 13(a) $d_{33} = 167 \times 10^{-12}$ m/V is used in the model calculation and it can be seen that the agreement is quite good.

The thickness electromechanical coupling constant k_t stays quite constant as predicted with slightly higher values. For information, the value of k_{33} for free vibrating PZT 7A rod (0.66) is also shown in the graph (Fig. 12(a)).

For the planar parameter calculations, $\bar{k}_p$ and $(\bar{s}_{11}^{E} + \bar{s}_{12}^{E})$ are shown in Figs. 14(a) (b), where $\bar{k}_p$ is found to be quite constant and varies from 0.29 to 0.33 for different volume fraction.

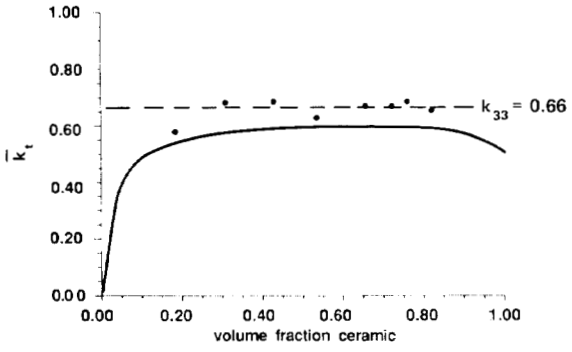

(a)

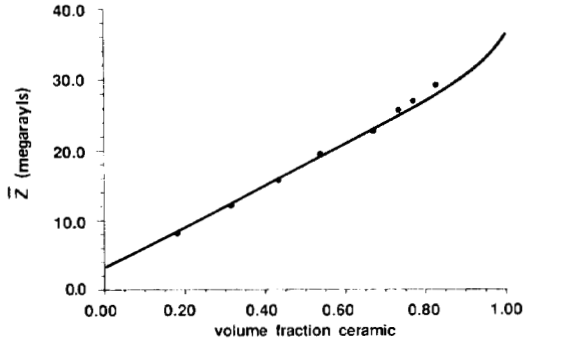

(b)

Fig. 12. (a) Experimental verification of variation of thickness coupling constant $\bar{k}_t$ with volume fraction of ceramic. (b) Experimental verification of variation of acoustic impedance $\bar{Z}$ with volume fraction of ceramic.

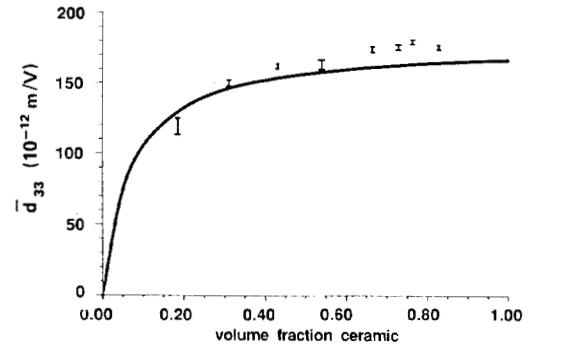

(a)

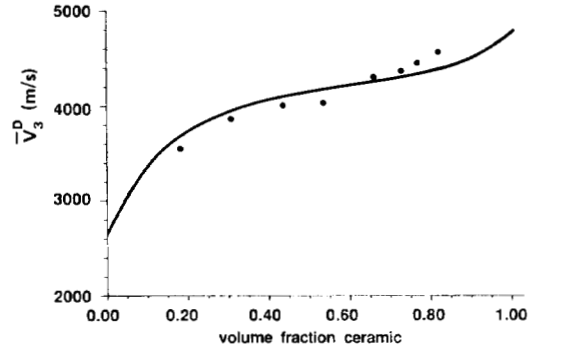

(b)

Fig. 13. (a) Experimental verification of variation of charge constant $\bar{d}_{33}$ with volume fraction of ceramic. (b) Experimental verification of variation of longitudinal velocity $\bar{V}_3^D$ with volume fraction of ceramic.

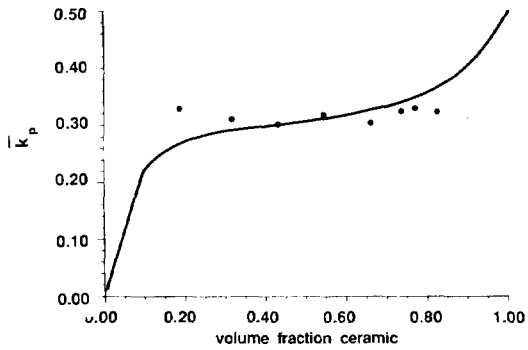

(a)

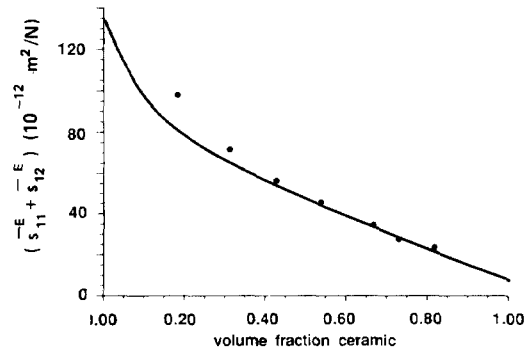

(b)

Fig. 14. (a) Experimental verification of variation of planar coupling constant k_p with volume fraction of PZT. (b) Experimental verification of the variation of compliance $\bar{s}^E_{11} + \bar{s}^E_{12}$ with volume fraction of PZT.

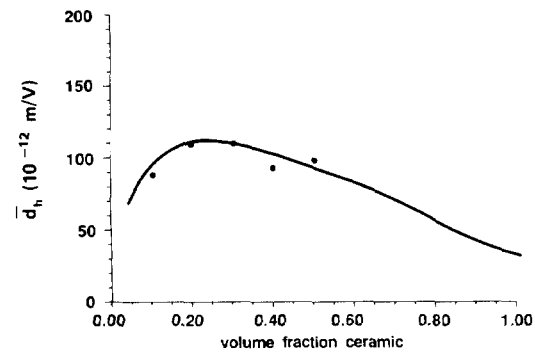

Fig. 15. PZT 5A/Spurr Epoxy 1-3 composite, $\bar{d}_h$ vs. ν, verification of the theory using result from [7].

Since the experimental set up for measuring $\bar{d}_h$ is unavailable, a different illustrative example will be used. The theoretical prediction using PZT 5A/Spurr Epoxy parameters [5] will be compared to the result (for 0.4 mm rod size) tabulated in Klicker's thesis [7, p. 107]. Fig. 15 shows that the experimental values agree quite well with the theory.

VII. Conclusion

Equations have been derived and presented that provide a framework for calculation of the essential ultrasonic parameters required for matching the electronic circuits to the composite transducer and prediction of the ultrasonic responses essential for ultrasonic transducer design.

Acknowledgment

The authors would like to thank Dr. T. Bui from Ausonics Pty. Ltd. and Dr. Y. S. Ng from Plessey Aust. Pty. Ltd. for their thoughtful comments and help. Thanks are also due to Mr. G. Hancock and Mr. Y. Tong of AWA Aust. Pty. Ltd. for their help in cutting the ceramics.

References

[1] R. E. Newnham, D. P. Skinner, and L. E. Cross, "Connectivity and piezoelectric-pyroelectric composites," *Mater. Res. Bull. 13*, pp. 525-536, 1978.

[2] T. R. Gururaja, W. A. Schulze, L. E. Cross, R. E. Newnham, B. A. Auld, and Y. J. Wang, "Piezoelectric composite materials for ultrasonic transducer applications. Part I: Resonant modes of vibration of PZT rod-polymer composites." *IEEE Trans. Sonics Ultrason.*, SU-32, pp. 481-498, 1985.

[3] T. R. Gururaja, W. A. Schulze, L. E. Cross, and R. E. Newnham, "Piezoelectric composite materials for ultrasonic transducer applications. Part II: Evaluation of ultrasonic medical applications." *IEEE Trans. Sonics Ultrason.*, SU-32, pp. 499-513, 1985.

[4] W. A. Smith, A. A. Shaulov, and B. M. Singer, "Properties of composite piezoelectric materials for ultrasonic transducers," in *Proc. 1984 IEEE Ultrason. Symp.*, pp. 539-544.

[5] W. A. Smith, A. Shaulov, and B. A. Auld, "Tailoring the properties of composite piezoelectric materials," in *Proc. 1985 IEEE Ultrason. Symp.*, pp. 642-647.

[6] D. P. Skinner, R. E. Newnham, and L. E. Cross, "Flexible composite transducers," *Mater. Res. Bull. 13*, pp. 599-607, 1978.

[7] K. A. Klicker, "Piezoelectric composite with 3-1 connectivity for transducer applications," Ph.D. Thesis, Solid State Science, The Pennsylvania State Univ., 1981.

[8] H. L. W. Chan, "Piezoelectric ceramic/polymer 1-3 composites for ultrasonic transducer applications," chap. 5, Ph.D. Thesis, Macquarie Univ., 1987.

[9] "IRE standard on piezoelectric crystal: Measurements of piezoelectric ceramics, 1961," in *Proc. IRE*, vol. 49, no. 7, 1961, pp. 1161-1169.

[10] *Guide to Dynamic Measurements of Piezoelectric Ceramics with High Electromechanical Coupling, Appendix A: Relationships between Material Constants*, IEC Standard 483 1976.

[11] N. M. Shorrocks, M. E. Brown, R. W. Whatmore, and F. W. Ainger, "Piezoelectric composites for underwater transducers," *Ferroelec.*, vol. 54, pp. 215, 1984.

[12] *Piezoelectric Ceramics Data Sheet*, Vernitron Ltd., 1969.

[13] *IEEE Standard on Piezoelectricity*, IEEE Standard 176, 1978.

Helen Lai Wah Chan was born in Hong Kong in 1948. She obtained B.Sc. and M.Phil. degrees in physics from the Chinese University of Hong Kong. She is a Ph.D. student at Macquarie University, Sydney, New South Wales, Australia, working on 1-3 piezoelectric ceramic/polymer composite for ultrasonic applications.

Joseph Unsworth (SM'80) was born in Bolton Lancashire, England in 1935. He obtained the National Certificate in chemistry, the B.Sc. (honors) degree in physics from University of Wales, City, Lountry, M.Sc. in electronics from University of Manchester, Institute of Science and Technology, and Ph.D. in Biophysics at Macquarie University, Sydney, New South Wales, Australia, where he is at present employed as an Associate Professor.

He is a Senior Member of IEEE, and Fellow of the Plastics & Rubber Institute, a Fellow of the Australian Institute of Physics, a Chartered Chemist and a Chartered Physicist.